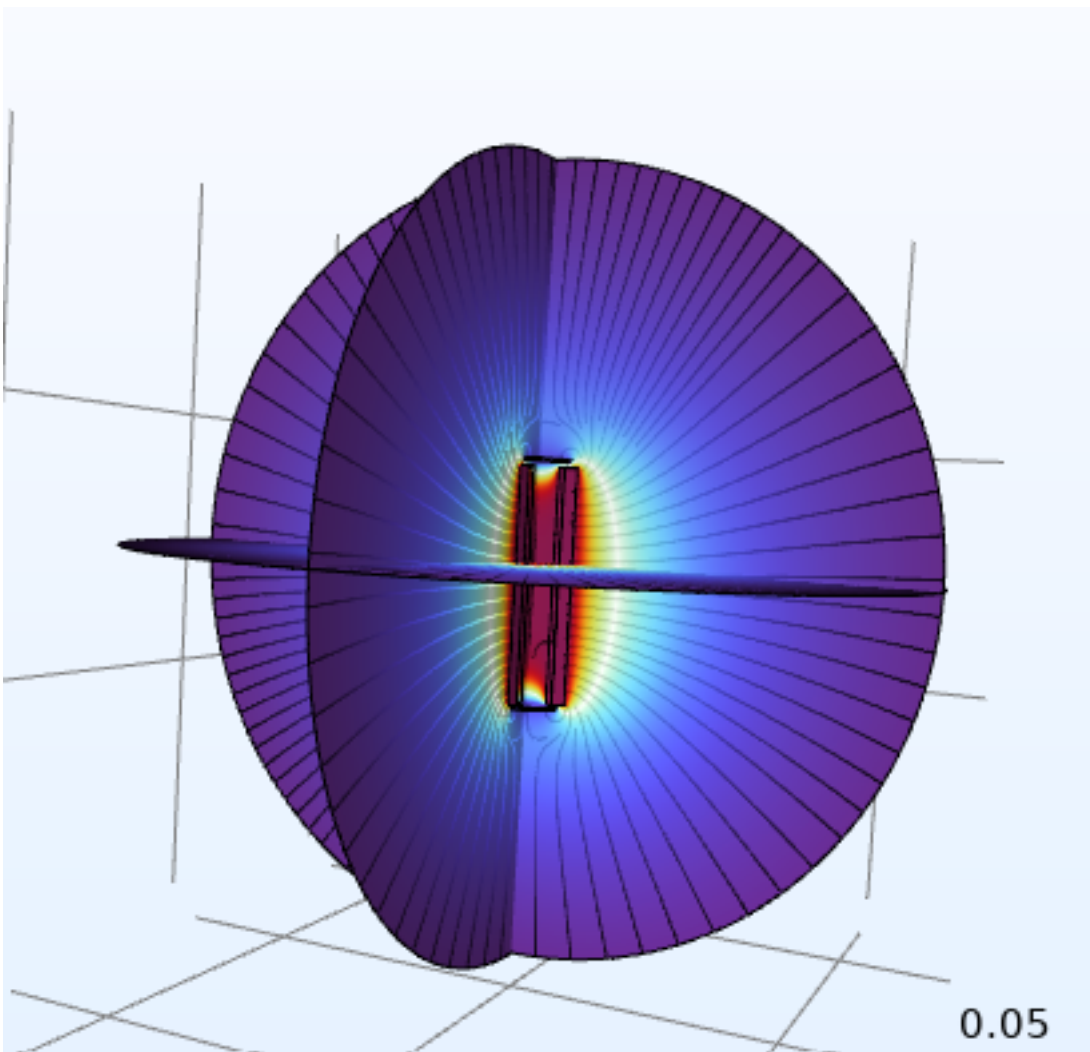


HardHaQ '25 Trapped Ion Problem Set Submission

Team Name: *Hard Nanos*
Members: *Nikhil, Rebanta, Lucas*

November 22 2025



1 Introduction

1.1 Problem Overview

The Ion Trap Challenge required us to modify an RF Paul trap to more effectively confine a single Yb^+ ion using the combination of an oscillating and a static electric field inside of a vacuum environment. The primary components of the trap are the RF rods for radial confinement, DC endcaps for axial stability, and a vacuum region to minimize ion collisions with background gas molecules.

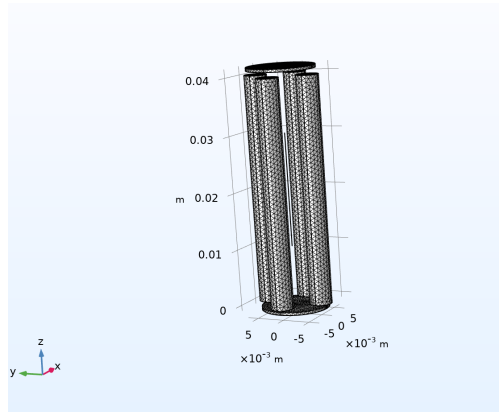


Figure 1: Schematic of the ion trap components: RF rods, DC endcaps, and vacuum chamber. Each component plays a crucial role in achieving stable ion confinement.

Our team adopted a systematic strategy to tackle the ion trap challenge. We began by developing a clear understanding of the fundamental components of the RF Paul trap, recognizing that each element plays a distinct and indispensable role in achieving stable confinement. This foundational knowledge ensured that subsequent modifications were grounded in physical intuition rather than trial and error.

1.2 RF Rods: Radial Confinement

The RF rods form the core of the quadrupole field. By applying an oscillating radiofrequency voltage, they generate a time-varying potential that counteracts the natural tendency of ions to escape. This produces dynamic stability in the radial plane through alternating focusing and defocusing forces.

The electrodes in a quadrupole ion trap cannot simply be held at static voltages. A purely static quadrupole potential would violate **Earnshaw's theorem**, which states that no arrangement of static electric fields can create a stable equilibrium point for a charged particle in free space. The quadrupole potential is given by

$$\Phi(x, y, z) = \frac{V}{2r_0^2}(x^2 - y^2),$$

where V is the applied voltage and r_0 is the characteristic electrode spacing. This configuration confines ions along one radial axis while defocusing them along the

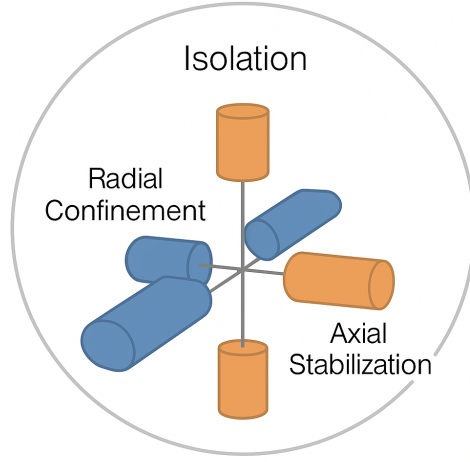


Figure 2: Schematic of RF Paul trap showing RF rods, DC endcaps, and vacuum chamber. Radial confinement arises from oscillating RF rods which produce a time-varying quadrupole potential that traps the Yb^+ ion dynamically in the radial plane.

orthogonal axis, producing a saddle-point potential that is inherently unstable.

To achieve confinement, the static voltages are replaced with an oscillating radio-frequency (RF) field. The rapid alternation between focusing and defocusing directions prevents the ion from escaping, and over many cycles the particle experiences an effective restoring force toward the trap center. This mechanism is analogous to the stabilization of the Kapitza pendulum, where fast oscillations create stability in an otherwise unstable system.

The time-averaged effect of the RF drive can be described by a **pseudo-potential**:

$$\Psi(r) = \frac{Q^2 V^2}{4m\Omega^2 r_0^2} r^2,$$

with Q the ion charge, m its mass, Ω the angular frequency of the RF drive, and r the radial displacement. This effective potential is quadratic in r , resembling a harmonic oscillator well. Its strength scales with V^2 and decreases with increasing m or Ω^{-2} , meaning heavier ions are harder to confine while higher-frequency drives enhance stability. In practice, trapped ions exhibit two types of motion: fast **micromotion** at the RF frequency and slower **secular motion** within the pseudo-potential well. The overall stability of trajectories is governed by the **Mathieu equations**, which define regions of confinement depending on the RF amplitude and frequency. This principle underlies devices such as the Paul trap and quadrupole mass filters, where precise tuning of the pseudo-potential enables selective confinement or ejection of ions based on their mass-to-charge ratio.

1.3 DC Endcaps: Axial Stability

While the RF field provides dynamic stabilization in the radial plane, it cannot prevent ions from drifting freely along the longitudinal (z) axis of the ion trap. To address this limitation, **DC endcap electrodes** are introduced. These electrodes establish a static

potential well along the trap axis, which provides axial confinement and completes the three-dimensional trapping scheme.

The axial potential can be expressed as

$$\Phi(z) = \frac{\kappa V_{DC}}{z_0^2} z^2,$$

where V_{DC} is the applied endcap voltage, z_0 is the characteristic axial dimension of the trap, and κ is a geometry-dependent constant that accounts for electrode shape and spacing. This quadratic form resembles a harmonic oscillator potential, providing a restoring force that confines ions toward the trap center.

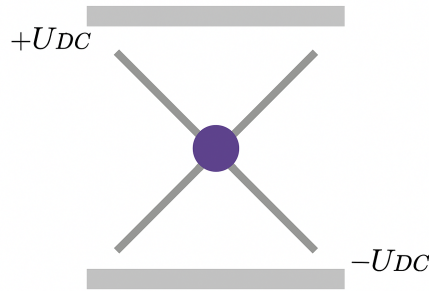


Figure 3: Illustration of DC endcaps providing axial confinement along the longitudinal axis of the trap. DC endcaps establish a static potential well along the trap axis, preventing axial drift and enabling long-term confinement when combined with the RF radial pseudopotential.

Physically, the DC endcaps play a complementary role to the RF field, as the RF drive ensures radial stability by generating a time-averaged pseudo-potential, while the DC endcaps supply a static potential that confines ions axially. Together, they create a three-dimensional trapping environment. In practice, the balance between RF and DC contributions must be carefully tuned. Too weak an endcap voltage leads to axial leakage, while excessive DC confinement can distort the radial pseudo-potential.

1.4 Vacuum Region: Isolation and Longevity

Surrounding the electrodes is the vacuum region, which is not merely a passive enclosure but a critical component of the ion trap system. Its primary function is to drastically reduce the number of background gas molecules that could interact with the trapped ion. In the absence of sufficient vacuum, residual gas atoms can collide with the ion, causing unwanted momentum transfer, decoherence, and heating — all of which degrade trap performance and reduce confinement time. These collisions are especially problematic in precision applications such as quantum computing or spectroscopy, where long coherence times and minimal environmental noise are essential.

The effectiveness of the vacuum is quantified by the mean free path λ , which represents the average distance an ion can travel before experiencing a collision. It is given by.

$$\lambda = \frac{k_B T}{\sqrt{2\pi d^2 P}},$$

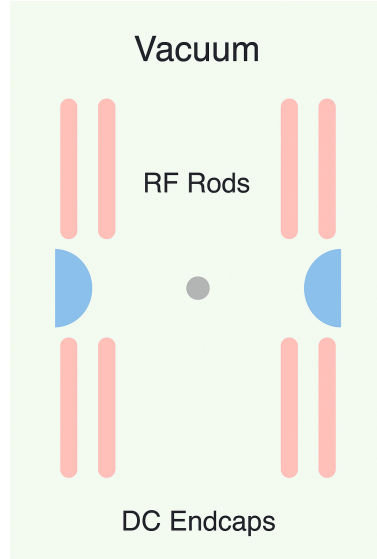


Figure 4: Diagram of mean free path in the vacuum region. Sparse background gas molecules increase the mean free path, reducing collisions and preserving ion coherence.

where k_B is Boltzmann's constant, T is the temperature, d is the effective diameter of the gas molecules, and P is the pressure. As pressure decreases, λ increases exponentially, meaning ions can traverse the trap volume without interference. Achieving ultra-high vacuum (UHV) conditions — typically below 10^{-9} Torr — ensures that λ is orders of magnitude larger than the trap dimensions, effectively suppressing ion loss due to scattering.

From an engineering standpoint, maintaining UHV requires careful material selection, surface treatment, and bake-out procedures to eliminate outgassing. The trap chamber must be sealed with low-permeability materials and equipped with high-efficiency pumps such as turbomolecular or ion pumps. These measures collectively ensure that the vacuum region supports stable, long-duration trapping, enabling high-fidelity measurements and reliable ion manipulation.

1.5 Interplay of Components

Together, these three components—RF rods for radial confinement, DC endcaps for axial stability, and the vacuum region for isolation, form a carefully balanced system. Each element addresses a limitation of the others: the RF rods alone cannot trap ions, the DC endcaps alone cannot prevent radial escape, and neither can function effectively without the vacuum.

Stable confinement emerges only when dynamic and static potentials are combined in a low-pressure environment, reflecting the fundamental design principle of the Paul trap. The oscillating RF field generates a pseudo-potential that stabilizes radial motion, while the DC endcaps create a static quadratic potential well along the longitudinal axis. The vacuum ensures that these forces act coherently over longer timescales.

Mathematically, the total potential experienced by an ion in the trap can be expressed as

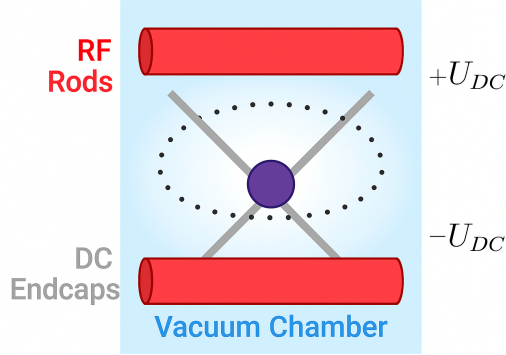


Figure 5: Composite schematic showing RF rods, DC endcaps, and vacuum chamber working together. Stable confinement emerges only when dynamic radial forces, static axial potentials, and isolation are combined.

the superposition of RF and DC contributions:

$$\Phi(x, y, z, t) = \Phi_{\text{RF}}(x, y, t) + \Phi_{\text{DC}}(z),$$

where

$$\Phi_{\text{RF}}(x, y, t) = \frac{V_{\text{RF}}}{2r_0^2}(x^2 - y^2) \cos(\Omega t), \quad \Phi_{\text{DC}}(z) = \frac{\kappa V_{\text{DC}}}{z_0^2} z^2.$$

This interplay is not just additive but synergistic: the RF and DC fields together establish a three-dimensional potential slope in which ions can be localized with high precision. The vacuum region amplifies this stability by extending ion lifetimes.

2 Mathematical Framework

2.1 Shorthand useful relations

The Mathieu parameter (radial) is

$$q = \frac{2QV}{mr_0^2\Omega^2}. \quad (1)$$

Here Q is the ion charge (C), m is the ion mass (kg), V is the RF peak amplitude (V), Ω is the RF angular frequency (rad s^{-1}), and r_0 is the characteristic trap radius (m). The secular frequency (radial secular motion) in the small- q limit is approximated by

$$\omega_{\text{sec}} \approx \frac{q}{2\sqrt{2}}\Omega = \frac{QV}{\sqrt{2}mr_0^2\Omega}. \quad (2)$$

2.2 Pseudopotential depth (U_{depth})

2.2.1 Governing formula

The time-averaged pseudopotential (in 1D radial coordinate r for an ideal quadrupole) is

$$\Psi(r) = \frac{Q^2}{4m\Omega^2} |\mathbf{E}_{\text{rf}}(r)|^2.$$

Here $\Psi(\mathbf{r})$ is the time-averaged pseudopotential (J). For the ideal quadrupole field amplitude $|\mathbf{E}_{\text{rf}}| \sim Vr/r_0^2$, this gives a quadratic pseudopotential:

$$\Psi(r) = \kappa \frac{Q^2 V^2}{4m\Omega^2 r_0^4} r^2,$$

so a characteristic *trap depth* (energy scale between center and effective boundary $r \sim r_0$) is commonly approximated as

$$U_{\text{depth}} \approx \kappa \frac{Q^2 V^2}{4m\Omega^2 r_0^2}. \quad (3)$$

Here U_{depth} denotes the trap depth (J) and κ is a dimensionless geometry factor (order unity). An alternative useful form in terms of the Mathieu parameter q is

$$U_{\text{depth}} = \kappa \frac{m\Omega^2 r_0^2}{16} q^2. \quad (4)$$

2.2.2 How each variable affects depth

- **RF amplitude V :** $U_{\text{depth}} \propto V^2$. Increasing V increases depth quadratically.
- **Drive frequency Ω :** $U_{\text{depth}} \propto 1/\Omega^2$. Increasing Ω reduces depth (inverse square).
- **Trap size r_0 :** $U_{\text{depth}} \propto 1/r_0^2$. Increasing r_0 decreases depth (inverse square).
- **Ion properties Q, m :** $U_{\text{depth}} \propto Q^2/m$. Higher charge increases depth; heavier mass decreases depth.
- **Geometry κ :** improves depth linearly with κ (ideal electrodes have $\kappa \approx 1$).

2.2.3 Practical remarks and trade-offs

- Increasing V increases q . Large q invalidates the pseudopotential approximation and increases micromotion.

2.3 Center offset (x_0) — static displacement and micromotion

2.3.1 Governing formula

If a stray DC electric field E_{dc} exists at the trap center, it exerts a force QE_{dc} on the ion. Balance this against the secular restoring force $m\omega_{\text{sec}}^2 x$ to obtain the static displacement (offset) x_0 :

$$x_0 = \frac{QE_{\text{dc}}}{m\omega_{\text{sec}}^2}. \quad (5)$$

where E_{dc} is the stray DC electric field (V/m) producing the static offset. Using the small- q expression for ω_{sec} ,

$$\omega_{\text{sec}} \approx \frac{QV}{\sqrt{2}mr_0^2\Omega},$$

we can express x_0 in terms of trap parameters:

$$x_0 \approx \frac{QE_{\text{dc}}}{m} \left(\frac{\sqrt{2}mr_0^2\Omega}{QV} \right)^2 = \frac{2mr_0^4\Omega^2}{QV^2} E_{\text{dc}}. \quad (6)$$

2.3.2 Excess micromotion amplitude (leading order)

For small q the amplitude of *excess* micromotion driven at RF frequency is approximately proportional to q times the static offset:

$$x_{\text{mm}} \approx \frac{q}{2} x_0. \quad (7)$$

Kinetic energy associated with excess micromotion scales as $\sim \frac{1}{2}m(\Omega x_{\text{mm}})^2$.

2.3.3 How each variable affects center offset

- **Stray field E_{dc} :** $x_0 \propto E_{\text{dc}}$ (linear). More stray field \Rightarrow larger offset.
- **Secular stiffness ω_{sec} :** $x_0 \propto 1/\omega_{\text{sec}}^2$. Stronger confinement (higher ω_{sec}) \Rightarrow smaller x_0 .
- **RF amplitude V :** Increasing V increases ω_{sec} (for fixed Ω and r_0) and thus reduces x_0 ; but increasing V also increases q and so multiplies offset into micromotion amplitude.
- **Drive frequency Ω :** Appears in ω_{sec} inversely; higher Ω (for fixed V) tends to reduce x_0 via ω_{sec} formula in practice.
- **Trap size r_0 :** Larger r_0 reduces secular frequency (for fixed V, Ω) so x_0 grows with r_0 .

2.3.4 Minimization strategies

- **Increase secular stiffness:** Raise V or reduce r_0 (within other constraints) to reduce x_0 .
- **Balance trade-offs:** Increasing V reduces x_0 but increases q (and thus micromotion amplitude $x_{\text{mm}} \propto qx_0$). Optimize to minimize residual micromotion energy.

2.4 RF power and power-per-depth (P/U_{depth})

2.4.1 Model for RF power

The RF power is modelled by the following equation extracted from the COMSOL file:

$$P_{\text{est}} = 10^3 \left(\omega_{\text{sec}} (\varepsilon \pi L) \frac{V_{\text{rf}}}{\sqrt{2}} \right)^2 \quad (8)$$

Here V_{rf} is the RF peak amplitude. In practice, P_{est} also depends on the effective electrode capacitance and series resistance of the RF drive and electrode structure (but, we assume it is negligible).

2.4.2 Power per depth

Combine (8) with the depth formula (3) which scales as $U_{\text{depth}} \propto V^2$. Eliminating V^2 yields:

$$\frac{P_{\text{est}}}{U_{\text{depth}}} \propto \frac{10^3 \left(\omega_{\text{sec}} (\varepsilon \pi L) \frac{V_{\text{rf}}}{\sqrt{2}} \right)^2}{\kappa \frac{m\Omega^2 r_0^2}{16} q^2} \Rightarrow \dots \Rightarrow \frac{P_{\text{est}}}{U_{\text{depth}}} \propto \frac{10^3 (\varepsilon \pi L)^2 V_{\text{rf}}^2}{\kappa m r_0^2}. \quad (9)$$

where the constant prefactor depends on the precise definitions used for U_{depth} and P_{est} ; the displayed scaling is the relevant design dependence.

2.4.3 How each variable affects P/U_{depth}

- **Trap size r_0 :** $P/U_{\text{depth}} \propto r_0^2$ (scales with trap area/size) — larger traps cost more power per depth.
- **Ion properties:** $P/U_{\text{depth}} \propto m/Q^2$ — heavier ions increase power per depth; higher ionic charge reduces it.
- **RF voltage V_{rf} :** $P/U_{\text{depth}} \propto V_{\text{rf}}^2$; smaller V_{rf} reduces power cost.
- **Electrode length L :** $P/U_{\text{depth}} \propto L^2$; smaller L reduces power cost if the quadrupole field quality is preserved.

2.4.4 Minimization of P/U_{depth}

1. **Choose moderate Ω :** Avoid excessively high drive frequencies unless required for stability/performance.
2. **Reduce r_0 where acceptable:** Smaller traps require less RF voltage for a given depth.

3 Optimization

3.1 Potential Approaches

There are two main strategies for optimizing the ion trap design: (1) modifying the geometries of the trap electrodes, and (2) adjusting the operating parameters such as voltages, frequencies, and characteristic dimensions of the RF Paul trap. Each approach offers distinct advantages and limitations.

Optimizing Operating Parameters Tuning parameters such as RF voltage amplitude, drive frequency, and endcap potentials is often the most accessible method of optimization.

- **Pros:**

- Rapid and flexible adjustments without requiring physical redesign of the trap.
- Enables fine control over stability regions defined by the Mathieu equations.
- Lower cost and shorter iteration cycles, since changes are implemented electronically.
- Useful for adapting a single trap geometry to different ion species or experimental conditions.

- **Cons:**

- Limited by the intrinsic geometry of the electrodes; cannot overcome fundamental design constraints.
- High voltages or frequencies may introduce technical challenges such as dielectric breakdown, heating, or increased micromotion.
- Optimization may be bounded by available electronics and power-handling capabilities.

Modifying Trap Geometries Altering electrode shapes, spacings, or overall trap dimensions provides a more fundamental route to optimization.

- **Pros:**

- Directly improves field uniformity and reduces anharmonicities in the pseudo-potential.

- Can expand stability regions and reduce sensitivity to parameter fluctuations.
- Enables custom designs tailored to specific applications (e.g., quantum computing, precision spectroscopy).

- **Cons:**

- Requires fabrication of new hardware, which is costly and time-consuming.
- Less flexible once built; geometry changes cannot be easily undone.
- Complex geometries may introduce alignment issues or machining tolerances that degrade performance.

Name	Expression	Value	Description
rod_radius	2[mm]	0.002 m	Radius of Rods
rod_length	50[mm]	0.05 m	Length of Rods
rod_spacing	5[mm]	0.005 m	Spacing from Centre
V_rf	300[V]	300 V	RF Voltage of Rods
V_dc	50[V]	50 V	DC Voltage of Rods
endcap_rad	6[mm]	0.006 m	Endcap Radius
endcap_thick	0.5[mm]	5E-4 m	Endcap Thickness
endcap_offset	1[mm]	0.001 m	Distance of Endcap from Trap
V_endcap	10[V]	10 V	DC Voltage of Endcap
f	10[MHz]	1E7 Hz	RF Frequency

Figure 6: Default operating parameters of the RF Paul trap. Initial voltages, frequencies, and dimensions set the baseline before any optimization.

Given the benefits of both optimizing values and geometries, our team elected to focus primarily on parameter optimization at the beginning of the challenge. This approach allowed us to rapidly iterate and explore a wide parameter space without the overhead of physical redesign. By leveraging computational tools to simulate trap performance under varying conditions, we could identify optimal settings that maximized trap depth, minimized offset, and controlled power consumption. Over the course of the challenge, we also explored geometric modifications to further enhance performance based on insights gained from our algorithmic parameter sweeps.

3.2 Optimizing Parameters

In our approach to optimizing the values of the parameters, we developed a Python script that interfaces with COMSOL's `mph` module to iteratively adjust key operating parameters of the ion trap model. The goal was to maximize trap depth while minimizing offset and power consumption, all within physically meaningful bounds. Because of the nature of the offset, minimizing it proved to be rather difficult, so the ratio of depth to power consumption was the main objective of the optimization script.

The script attempts to optimize physical parameters of an ion trap model in COMSOL by coupling the `mph` Python interface with SciPy's `minimize` routine. The workflow can be summarized as follows:

- **Baseline, Targets, and Weights:** Baseline values are taken from the COMSOL GUI and serve as the starting point. Target values specify desired outcomes (e.g., trap depth ≥ 5 eV, offset ≈ 0 mm, power ≈ 10 mW). Each objective is assigned a weight to reflect its relative importance, and each objective is designed to be just beyond what we thought was realistically achievable.
- **Bounds:** Each parameter is constrained to physically meaningful ranges (e.g., $0 \leq V_{rf} \leq 1000$, $10^6 \leq f \leq 10^8$). These bounds are used to normalize parameters into the unit cube $[0, 1]^n$ for optimization and then denormalize them back to physical units before evaluation.
- **Objective Function:** The function computes normalized scores relative to targets:

$$\text{depth score} = \frac{\text{depth}}{\text{target depth}}, \quad \text{offset score} = \frac{\text{target offset}}{\text{actual offset}}, \quad \text{power score} = \frac{\text{target power}}{\text{actual power}}.$$

These are combined into a weighted sum. Higher scores indicate better performance.

- **Trial Execution:** For each candidate parameter set, values are pushed into the COMSOL model, the study is solved, and metrics such as trap depth, offset, and power are extracted. Penalties are applied if results are unphysical. The optimizer minimizes the negative score, effectively maximizing performance.
- **Optimization Loop:** The Nelder–Mead algorithm iteratively proposes new parameter sets in normalized space, evaluates them via COMSOL, and updates its simplex until convergence or iteration limits are reached.
- **Logging:** Each trial's parameters and results are written to a CSV file for record-keeping and more in-depth analysis.

In summary, the script establishes a simulation-driven optimization loop:

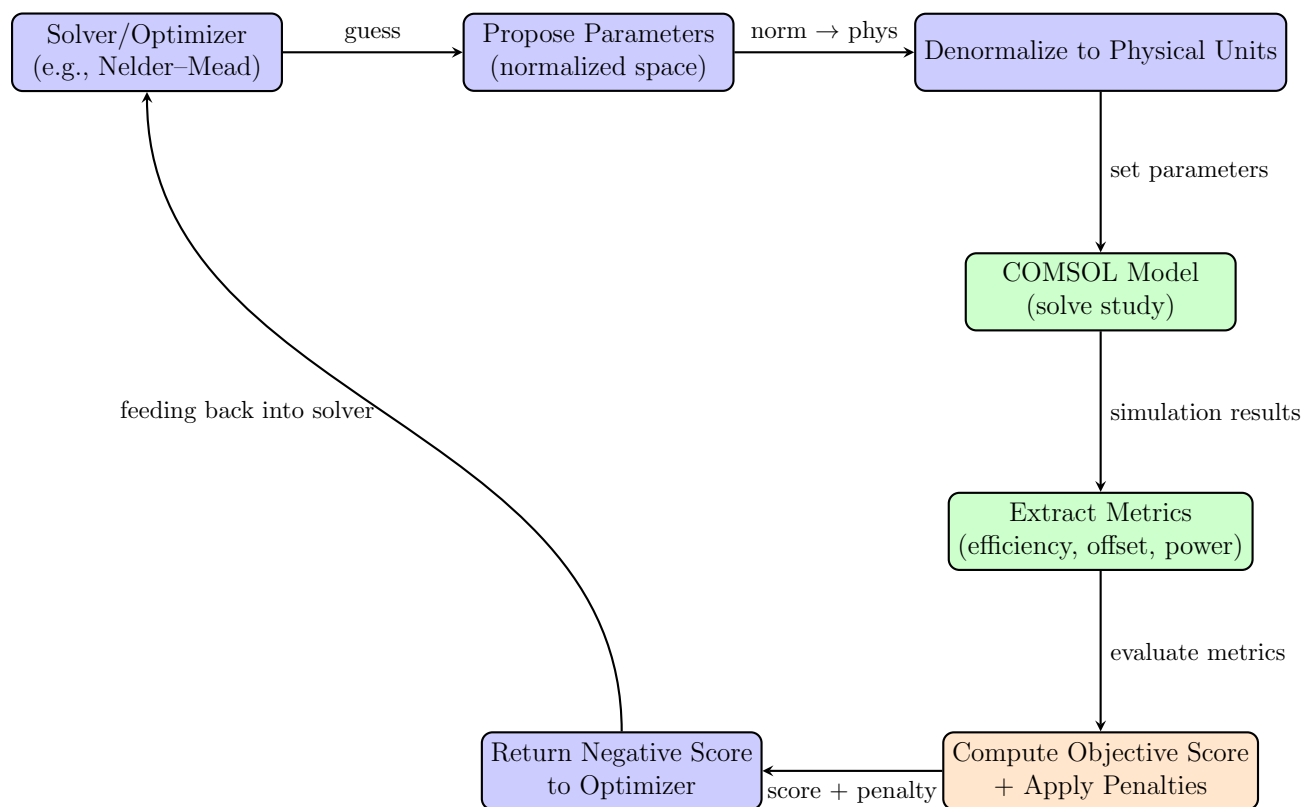


Figure 7: simulation-driven optimization loop using SciPy and COMSOL. Parameters are proposed, evaluated, and scored before looping back.

3.3 Geometric Modification

In addition to parameter optimization, we explored modifications to the electrode geometry itself. The change we ultimately attempted to implement was a reshaping of the electrodes into an hourglass profile. By tapering the electrode structure, the constriction is supposed to generate additional vertical confinement forces that pushes the ion inward along the z -axis. The intended effect of this is to provide direct assistance to the endcap electrodes in minimizing axial motion.

The hourglass geometry also was intended to assist in reducing offset. Its symmetric focusing of the pseudo-potential toward the trap center conceptually would help stabilize the ion's position while maintaining radial uniformity.

Unfortunately, we were unable to fully implement and test this geometric modification within the COMSOL environment. However, we believe that such geometric changes hold promise for further enhancing trap performance beyond what parameter tuning alone can achieve.

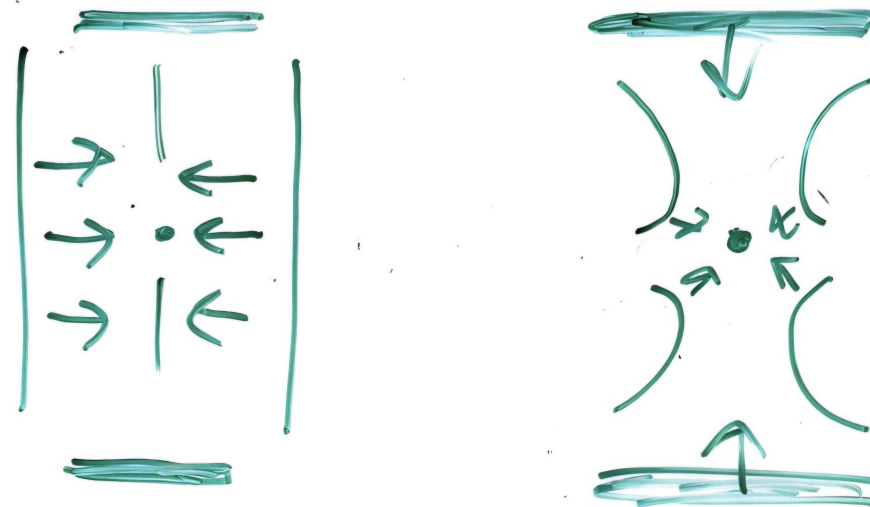


Figure 8: Pictured above is a conceptual rendering of the hourglass electrode geometry. The tapered design aims to enhance axial confinement and reduce offset by focusing the pseudo-potential toward the trap center.

4 Conclusion

Through parameter optimization, our team achieved a final Trap Metrics table with the following key results:

Table 1: Optimization Results for Ion Trap Parameters

V_rf	V_dc	V_endcap	rod_spacing	rod_radius	rod_length	endcap_offset	endcap_rad	endcap_thick	f
0.3887	76.5038	8.3279	0.00586	0.00179	0.04221	0.00096	0.00608	0.00052	9514109.64

Table 2: Trap Metrics from COMSOL Global Evaluation

depth_eV	minU_eV	maxU_eV	trap_x	trap_y	trap_z	offset_mm	P_est_mW
0.9755	74.3162	75.2917	0	-5.0E-6	0.01	10.0000	0.01083

These results reflect an incredible improvement over the baseline configuration, demonstrating the effectiveness of our optimization strategy in enhancing trap performance without geometrically changing the electrode structure.

- Exported Trap Metrics table (.txt file)
- Screenshot(s) of geometry and potential distribution
- Modified COMSOL file (.mph)
- Written summary (this document)